Airway epithelial innate host defence in chronic obstructive pulmonary disease

Amatngalim, G.D.

CHAPTER 3

Basal cells contribute to innate immunity of the airway epithelium through production of the antimicrobial protein RNase 7.

Gimano D. Amatngalim [1], Yolanda van Wijck [1], Yvonne de Mooij-Eijk [1], Renate M. Verhoosel [1], Jürgen Harder [2], Annemarie N. Lekkerkerker [3], Richard A.J. Janssen [3], Pieter S. Hiemstra [1]

[1] Department of Pulmonology, Leiden University Medical Center, Leiden, The Netherlands
[2] Department of Dermatology, University Hospital Schleswig-Holstein, Kiel, Germany
[3] Galapagos B.V., Leiden, The Netherlands

The Journal of Immunology. 2015 Apr 1;194(7):3340-50.

ABSTRACT

Basal cells play a critical role in the response of the airway epithelium to injury and are recently recognized to also contribute to epithelial immunity. Antimicrobial proteins and peptides are essential effector molecules in this airway epithelial innate immunity. However, little is known about the specific role of basal cells in antimicrobial protein and peptide production and about the regulation of the ubiquitous antimicrobial protein RNase 7. In this study, we report that basal cells are the principal cell type producing RNase 7 in cultured primary bronchial epithelial cells (PBEC). Exposure of submerged cultured PBEC (primarily consisting of basal cells) to the respiratory pathogen nontypeable *Haemophilus influenzae* resulted in a marked increase in expression of RNase 7, although this was not observed in differentiated air-liquid interface cultured PBEC. However, transient epithelial injury in air liquid interface–cultured PBEC induced by cigarette smoke exposure led to epidermal growth factor receptor–mediated expression of RNase 7 in remaining basal cells. The selective induction of RNase 7 in basal cells by cigarette smoke was demonstrated using confocal microscopy and by examining isolated luminal and basal cell fractions. Taken together, these findings demonstrate a phenotype-specific innate immune activity of airway epithelial basal cells, which serves as a second line of airway epithelial defence that is induced by airway epithelial injury

INTRODUCTION

Mucosal epithelial cells are an essential component of the host defense barrier against microbial pathogens. In the lung, a pseudostratified layer of airway epithelial cells provides this host defense via a passive barrier function but also active innate immune defense mechanisms (1, 2). These mechanisms are primarily executed by airway epithelial luminal cells (LCs), mainly composed of ciliated and secretory cells, which facilitate for instance mucociliary clearance, defense mediated by periciliary tethered mucins, production of innate immune mediators upon pathogen recognition, and Ig transcytosis toward the airway surface liquid (3-6). In contrast to LCs, it has been largely unexplored whether airway epithelial basal cells (BCs) have an innate immune function. BCs are characterized as epithelial progenitor cells and defined based on the expression of p63 and cytokeratin 5 (KRT5) (7-9). BCs display a low turnover at normal homeostatic conditions but rapidly expand and subsequently differentiate toward other epithelial phenotypes upon injury to restore the airway epithelial barrier. The basolateral localized BCs are shielded from direct microbial contact by the overlying LCs in intact airway epithelium. However, airway epithelial injury caused by disruption of the epithelial barrier because of the loss of cell–cell contact or shedding of LCs after extensive injury may increase microbial exposure. This may enhance the vulnerability of BCs and underlying tissues to respiratory infections. Recently, Byer *et al.* (10) demonstrated selective expression of the pro-inflammatory mediator IL-33 by a subpopulation of BCs in patients with chronic obstructive pulmonary disease. On the basis of this observation, we speculate that BCs might display other unique innate immune responses, which act as a second line of airway epithelial host defense in addition to the activity of LCs. Antimicrobial proteins and peptides (AMPs) are important innate immune mediators involved in airway epithelial host defense (11). AMPs display direct antimicrobial activity against bacteria, viruses, and fungi but also exhibit immunomodulatory and wound healing properties (12, 13). The antimicrobial RNase 7 is a secreted RNase A family member displaying antimicrobial activity toward a range of pathogens, including the respiratory pathogen *Pseudomonas aeruginosa* (14-16). Previous studies exploring the regulation of RNase 7 expression in skin, urinary tract, and ocular surface epithelial cells, demonstrated increased RNase 7 expression upon stimulation with microbes, microbial compounds, and pro-inflammatory cytokines (17-19). Moreover, mechanical injury and UV radiation induce expression of RNase 7 in keratinocytes (20, 21), demonstrating that epithelial injury is a potent inducer of RNase 7 expression. Although RNase 7 expression has been detected in cultured airway epithelial cells (14), it is currently unknown how RNase 7 expression is regulated in these cells. In this paper, we provide evidence that BCs are the principal cell producing RNase 7 in cultured human primary bronchial epithelial cells (PBEC) upon exposure to the respiratory pathogen nontypeable *Haemophilus influenzae* (NTHi) and epithelial barrier disruption caused by cigarette smoke exposure. Submerged cultured undifferentiated PBEC (S-PBEC), primarily consisting of BCs, but not mucociliary differentiated air-liquid interface–cultured PBEC (ALI-PBEC), expressed RNase 7 upon stimulation with UV-inactivated NTHi. Transient epithelial injury induced by whole cigarette smoke coincides with epidermal growth factor receptor (EGFR)–dependent expression of RNase 7 in ALI-PBEC, and this expression is specifically observed in BCs. These findings demonstrate a novel innate immune defense function of BCs, which act as a second line of airway epithelial defense induced upon injury.

MATERIALS AND METHODS

Bronchial epithelial cell culture

Human PBEC were isolated from tumour-free resected lung tissue from anonymous donors by enzymatic digestion as reported previously (22). Mucociliary-differentiated ALI-PBEC were cultured as previously described (23), using semipermeable Transwell membranes with a 0.4-mm pore size (Corning Costar, Cambridge, MA). Transwells were coated with a mixture of 30 µg/ml PureCol (Advanced BioMatrix, San Diego, CA), 10 µg/ml BSA (Sigma-Aldrich, St. Louis, MO), and 10 µg/ml fibronectin (isolated from human plasma) diluted in PBS, at 37°C, 5% CO_2 for 2–24 h. PBEC (passage 2) were seeded on coated Transwells at a density of 40,000 cells and cultured in submerged condition using a 1:1 mixture of DMEM (Life Technologies, Bleiswijk, the Netherlands) and bronchial epithelial growth medium (Lonza, Verviers, Belgium) (B/D medium) with supplementation of BEGM BulletKit singlequots (0.4% [w/v] bovine pituitary extract, 1 mM hydrocortisone, 0.5 ng/ml human hEGF, 0.5 µg/ml epinephrine, 10 µg/ml transferrin, 5 µg/ml insulin, T3, and 0.1 ng/ml retinoic acid) (Lonza), 1 mM HEPES (Lonza), 1 mg/ml BSA (Sigma-Aldrich), 100 U/ml penicillin and 100 µg/ml streptomycin (Lonza), and additional supplementation of 15 ng/ml retinoic acid (Sigma-Aldrich) to induce mucociliary differentiation. After reaching confluence (~ 4–5 d), cells were cultured air exposed for an additional period of 2 wk before use. Undifferentiated S-PBEC were cultured in 12-well tissue culture plates in B/D medium including supplements as earlier described but without additional retinoic acid supplementation. Upon reaching 80–90% confluence, S-PBEC were used for further experiments.

NTHi

NTHi strain D1 (24) was cultured on chocolate agar plates (bioMérieux, Craponne, France) at 5% CO_2 and 37°C overnight. A selected colony was resuspended in 10 ml Tryptone soya broth + X- and V-factor (Mediaproducts BV, Groningen, the Netherlands) and incubated at 37°C while shaking overnight. Next, 1 ml of the overnight broth containing NTHi was transferred into new 10 ml Tryptone soya broth + X- and V-factor and incubated for 3 h at 37°C while shaking. Afterward, the bacteria containing broth was centrifuged for 10 min at 3000 rpm, and the pellet was washed with PBS. The bacterial pellet was resuspended in PBS after an additional washing step, and the concentration was adjusted to an OD_{600} 1 (1 x 10^9 CFU/ml). The NTHi was subsequently inactivated by UV exposure for 2 h.

Whole cigarette smoke exposure and other stimuli

ALI-PBEC were exposed to cigarette smoke using 3R4F reference cigarettes (University of Kentucky, Lexington, KY) in a whole smoke exposure model adapted from Beisswenger *et al.* (25) as depicted in Figure 2A. ALI-PBEC were placed into modified hypoxic chambers (Billups Rothenberg, Del Mar, CA), further referred to as exposure chambers, localized inside an incubator at 37°C and 5% CO_2. Next mainstream smoke derived from one cigarette or air as negative control was infused inside respectively a "Smoke" and "Air" exposure chamber by a mechanical pump using a continuous flow of 1 l/minute for a period of 4–5 min. A ventilator inside the exposure chambers equally distributed and mixed the infused air/smoke with humidified warm air derived from the incubator to prevent inflammatory responses by PBEC as reported previously (25). After exposure, residual smoke inside the exposure chamber was

removed for a period of 10 min by flushing the chambers with air derived from the incubator. The amount of smoke infused inside the exposure chamber was measured by determining the weight difference of a filter placed between the pump and exposure chamber before and after exposure. Approximately 2 mg cigarette smoke–derived particles were deposited on the filter as determined by measuring the filter of different exposures. After smoke or air exposure, the culture medium of ALI-PBEC was refreshed, and cells were incubated at 37°C and 5% CO_2 for the indicated period of times. UV-inactivated NTHi or Pam3CSK4 (InvivoGen, San Diego, CA) was administered in a volume of 100 µl in PBS at the apical surface of ALI-PBEC or added to the culture medium when stimulating S-PBEC. To examine cell signalling pathways, the following chemical inhibitors were applied: AG1478, anti-EGFR neutralizing Ab, and U0125 (all Calbiochem, Darmstadt, Germany). Inhibitors were added into the basal culture medium and pre-incubated for 1 h prior to smoke exposure. Stimulation of ALI-PBEC with rTGF-α (PeproTech, Rocky Hill, NJ) was done by adding this growth factor to the culture medium. In confocal imaging and FACS experiments, 5 µg/ml brefeldin A (Sigma-Aldrich) was added in the culture medium to prevent protein secretion.

Cell cytotoxicity and viability assays

Lactate dehydrogenase (LDH) release in the apical surface liquid, collected by washing the epithelial cultures apical with 100 µl PBS, and culture medium was assessed using a cytotoxicity detection kit (Roche, Basel, Switzerland), according to the manufacturer's protocol. One hundred microliters of 0.1% (v/v) Triton X-100 in PBS was applied on the apical surface as positive control. The transepithelial electrical resistance (TEER) was measured using the MilliCell-ERS (Millipore, Bedford, MA). Cell permeability was determined by the FITC–dextran permeability assay. In this assay, 1 mg/ml FITC–dextran (4 kDa; Sigma-Aldrich) diluted in PBS was added to the apical side and incubated for 2 h. Next, 100 µl of the basal culture medium was transferred into solid black 96-well plates (Costar-Corning), and the fluorescence was measured with an excitation/emission wavelength of 490/521 nm using a Wallac Victor 2 Microtiter Plate Reader (PerkinElmer, Waltham, MA).

RNA isolation, reverse transcription, and quantitative real-time PCR

Total RNA was isolated using the miRNeasy Mini Kit (Qiagen, Venlo, the Netherlands) following the manufacturer's protocol, and RNA quantities were measured using the Nanodrop ND-1000 UV-visible (UV-Vis) spectrophotometer (Nanodrop Technologies, Wilmington, DE). cDNA synthesis was performed by RT-PCR of 1 µg RNA reverse mixed with oligo (deoxythymidine) primers (Qiagen) and Moloney murine leukemia virus polymerase (Promega, Leiden, The Netherlands) at 37°C. Quantitative PCR (qPCR) was performed using IQ Sybr green supermix (Bio-Rad) and a CFX-384 real-time PCR detection system (Bio-Rad). Reactions were performed using the primers indicated in Table 1. The housekeeping genes RPL13A and ATP5B were selected using the "Genorm method" (Genorm; Primer Design, Southampton, U.K.). Bio-Rad CFX manager 3.0 software (Bio-Rad) was used to calculate arbitrary gene expression by using the standard curve method.

Table 1. Primer sequences

Gene	Forward primer	Reverse primer
RNASE7	5'-CCAAGGGCATGACCTCATCAC-3'	5'-ACCGTTTTGTGTGCTTGTTAATG-3'
IL8	5'-CAGCCTTCCTGATTTCTG-3'	5'-CACTTCTCCACAACCCTCTGC-3'
IL6	5'-CAGAGCTGTGCAGATGAGTACA-3'	5'-GATGAGTTGTCATGTCCTGCAG-3'
DEFB4	5'-ATCAGCCATGAGGGTCTTG-3'	5'-GCAGCATTTTGTTCCAGG-3'
CCL20	5'-GCAAGCAACTTTGACTGCTG-3'	5'-TGGGCTATGTCCAATTCCAT-3'
LCN2	5'-CCTCAGACCTGATCCCAGC-3'	5'-CAGGACGGAGGTGACATTGTA-3'
FOXJ1	5'-GGAGGGGACGTAAATCCCTA-3'	5'-TTGGTCCCAGTAGTTCCAGC -3'
MUC5AC	5'-ATTTTTTCCCCACTCCTGATG-3'	5'-AAGACAACCCACTCCCAACC-3'
TP63	5'-CCACCTGGACGTATTCCACTG-3'	5'-TCGAATCAAATGACTAGGAGGGG-3'
KRT5	5'-CCAAGGTTGATGCACTGATGG-3'	5'-TGTCAGACATGCGTCTGC-3'
RPL13A	5'-AAGGTGGTGGTCGTACGCTGTG-3'	5'- CGGGAAGGGTTGGTGTTCATCC-3'
ATP5B	5'-TCACCCAGGCTGGTTCAGA-3'	5'-AGTGGCCAGGGTAGGCTGAT-3'

Sequences of primers used for qPCR.

ELISA

Protein secretion by ALI-PBEC was determined in the apical surface liquid and in the basal medium. The secretion of IL-8 was determined by ELISA following the manufacturer's protocol (Sanquin, Amsterdam, The Netherlands). RNase 7 secretion was assessed by ELISA as described previously (16). The OD values were measured with a microplate reader (Bio-Rad).

Isolation of luminal and basal airway epithelial cells

The basal and luminal fraction of ALI-PBEC were isolated according to a method adapted from Jakiela *et al.* (26). Cultured ALI-PBEC were washed twice with calcium-free PBS. Next, calcium-free MEM (Life Technologies) was applied to the apical side (700 µl) and the basolateral compartment to break down the integrity of the intercellular junctions. This was monitored by TEER measurements, which reached background levels after ~15–20 min. Next, the apical medium was substituted by 700 µl Trypsin Versene (Lonza) and incubated for 7–10 min until luminal cells started to detach. The detached luminal fraction was collected, and the apical surface was subsequently washed twice gently with 700 µl DMEM supplemented with 5% heat-inactivated FCS (Life Technologies). The cells that were collected by this washing step were added to the luminal fraction, which was then centrifuged for 7 min at 1200 rpm. After removal of the supernatant, mRNA was isolated from the cell pellet (luminal fraction) and the epithelial cells that remained attached to the inserts (basal fraction).

Immunofluorescence staining and confocal imaging

For immunofluorescence staining, ALI-PBEC were fixed in 4% paraformaldehyde, permeabilized in 0.3% (v/v) Triton X-100 in PBS, and blocked in blocking solution consisting of 5% (w/v) BSA and 0.3% (v/v) Triton X in PBS. All incubation steps were 30 min at room temperature and contained washing steps with PBS in-between. Membranes containing ALI-PBEC were detached from the Transwell using a razorblade and transferred to 24-well tissues

culture plates for Ab staining. The primary Abs (mouse mAb against RNase 7 and rabbit mAb against p63 [Abcam, Cambridge, U.K.]) were diluted in blocking solution and added to the cells for 1 h at room temperature. The secondary Abs goat anti-mouse Alexa Fluor 488, goat anti-rabbit Alexa Fluor 568 (both Invitrogen), and DAPI, diluted in blocking buffer, were added to the cells for 30 min at room temperature in the dark. Next, the PBEC-containing membranes were placed on coverslips and mounted in Vectashield Hard Set Mounting Medium (Vector Labs, Burlingame, CA). Confocal images were taken using a Leica TCS SP5 confocal inverted microscope (Leica Microsystems, Wetzlar, Germany) and processed using the Leica Application Suite Advanced Fluorescence software (Leica Microsystems).

Flow cytometry

ALI-PBEC were detached from the Transwell by trypsinization using soft trypsin, consisting of 0.3 mg/ml trypsin 250 (BD Biosciences, San Jose, CA), 0.1 mg/ml EDTA, 1 mg/ml glucose (both BDH Chemicals, Poole, U.K.), 100 U/ml penicillin, and 100 μg/ml streptomycin in PBS (pH 7.45). Trypsinization was stopped using 1.1 mg/ml soy bean trypsin inhibitor (Sigma-Aldrich) in keratinocyte serum-free medium (Life Technologies). Cells were washed once in cold PBS and stained with live/dead stain aqua (Invitrogen). Then, cells were washed in PBS, permeabilized using 0.5% (v/v) saponin (Sigma-Aldrich) in PBS for 5 min on ice, and fixed with 3.9% (v/v) formaldehyde (Merck) in PBS for 15 min at room temperature. Next, primary Abs (mouse mAb against RNase 7 [Abcam, Cambridge, U.K.] and rabbit polyclonal Ab against KRT5 [Santa Cruz Biotechnology, Santa Cruz, CA]) were added, followed by secondary Ab treatment (goat anti-mouse Alexa Fluor 488 and goat-anti-rabbit Alexa Fluor 647 [both Invitrogen]), both diluted in 0.5% saponin supplemented with human FcR binding inhibitor (eBioscience, San Diego, CA). Both primary and secondary Abs were incubated for 30 min at room temperature. Cells were measured on a FACSCanto II (BD Biosciences), and analysis was performed using FlowJo (version 7.6.5) software (Tree Star, Ashland, OR). Gates were placed according to unstained and single stains with secondary Abs (Supplementary Figure 1).

SDS-PAGE and Western blot

SDS-PAGE gel electrophoresis and Western blotting was performed as described previously (27). In short, PBEC were washed with ice-cold washing buffer consisting of 5 mM Tris (pH 6.4), 100 mM NaCl, 1 mM $CaCl_2$, and 1 mM $MgCl_2$, and cell lysates were prepared in lysis buffer consisting of 0.5% (v/v) Triton X-100, 0.1 M Tris-HCl (pH 7.4), 100 mM NaCl, 1 mM $MgCl_2$, 1 mM $CaCl_2$ 1 mM Na_3VO_4, and protease inhibitor mixture (Roche) and subsequently suspended in SDS-PAGE sample buffer consisting of 4% (w/v) SDS, 10% (v/v) 2-ME, 20% (v/v) glycerol, 0.5 M Tris (pH 6.8), and 0.003% (w/v) Bromophenol blue. SDS-gel electrophoresis was conducted using 10–12.5% glycine-based gels, and afterward, separated proteins were transferred to polyvinylidene difluoride membranes. Membranes were blocked with blocking buffer consisting of 5% (w/v) skim milk (Sigma-Aldrich) in PBS/0.05% (v/v) Tween 20 and incubated with primary Abs (rabbit polyclonal Ab ERK1/2, p-ERK1/2, p-EGFR, and mouse mAb b-actin [all Cell Signaling Technology, Leiden, The Netherlands], mouse mAb EGFR [BD Biosciences], and mouse mAb RNase 7 [Abcam]) in 5% (w/v) BSA TBS/0.05% (v/v) Tween 20 overnight at 4°C. Afterward, membranes were incubated with secondary HRP-labelled Ab (Sigma-Aldrich) in blocking buffer for 1 h, and membranes were subsequently

developed with ECL substrate (ThermoScientific, Rockford, IL). Results were analysed by densitometry using Adobe Photoshop (Adobe Systems, San Jose, CA).

Statistical analysis

Graphs were made and statistical analysis was performed in GraphPad PRISM 6.0 (GraphPad Software, La Jolla, CA). Data are shown as means ± SEM. Differences were considered significantly different with $p<0.05$ explored by (un)paired Student t test or one/two-way ANOVA as appropriate.

RESULTS

NTHi increases expression of RNase 7 in undifferentiated S-PBEC but not in mucociliary differentiated ALI-PBEC

We first investigated whether the common respiratory pathogen NTHi induced RNase 7 expression in cultured PBEC. Therefore, undifferentiated S-PBEC were exposed to UV-inactivated NTHi for 6 and 24 h, and RNase 7 expression was assessed by qPCR. The results showed that NTHi induced RNase 7 mRNA expression by S-PBEC after 24 h but not 6 h of stimulation (Figure 1A). In contrast, mRNA expression of the well-defined bacterial-induced antimicrobial peptide human β-defensin-2 (hBD-2) was increased by NTHi both at 6 and 24 h. As shown by others (28), we observed that undifferentiated S-PBEC primarily consist of p63+ BCs (*data not shown*). Because mucociliary-differentiated ALI-PBEC are more comparable to the pseudostratified airway epithelium *in vivo* (29), we subsequently compared RNase 7 mRNA expression in ALI-PBEC and S-PBEC. Interestingly, ALI-PBEC did not display an increase in RNase 7 mRNA in response to various concentrations of NTHi after 24 h of stimulation, whereas dose-dependent induction was observed in S-PBEC (Figure 1B). In contrast, a dose-dependent NTHi-induced expression of hBD-2 was observed in both ALI- and S-PBEC. Further evaluation of the expression of other innate immune mediators demonstrated that NTHi induced mRNA expression of IL-8, IL-6, CCL20, and lipocalin 2 (LCN2) in both S-PBEC and ALI-PBEC (Figure 1C). To explore baseline RNase 7 expression during mucociliary differentiation, mRNA levels of RNase 7 were measured in S-PBEC and in ALI-PBEC at 1 and 2 wk after initial air exposure. Compared with S-PBEC, no difference in mRNA levels was observed in ALI-PBEC cultured 1 wk in air exposed conditions, whereas after 2 wk a significant decrease in RNase 7 mRNA was observed (Figure 1D). As expected, airway epithelial cell differentiation furthermore resulted in a decreased mRNA expression of the BC marker p63 and increased expression of ciliated and goblet cell markers, respectively, FOXJ1 and MUC5AC. These findings suggest, that in contrast to other examined innate immune mediators, RNase 7 is selectively produced by airway BCs but not by mucociliary-differentiated airway epithelial cells at baseline conditions and upon NTHi stimulation.

Cigarette smoke–induced transient epithelial injury results in induction of RNase 7 in ALI-PBEC

BCs display enhanced activity upon injury, and it has been demonstrated that injury induces RNase 7 expression in keratinocytes (7, 20, 21). Therefore, we hypothesized that injury of ALI-PBEC can reinitiate expression of RNase 7 by remaining undifferentiated BCs. Cigarette smoke is a well-known inhaled toxic mixture that induces airway epithelial injury (30, 31).

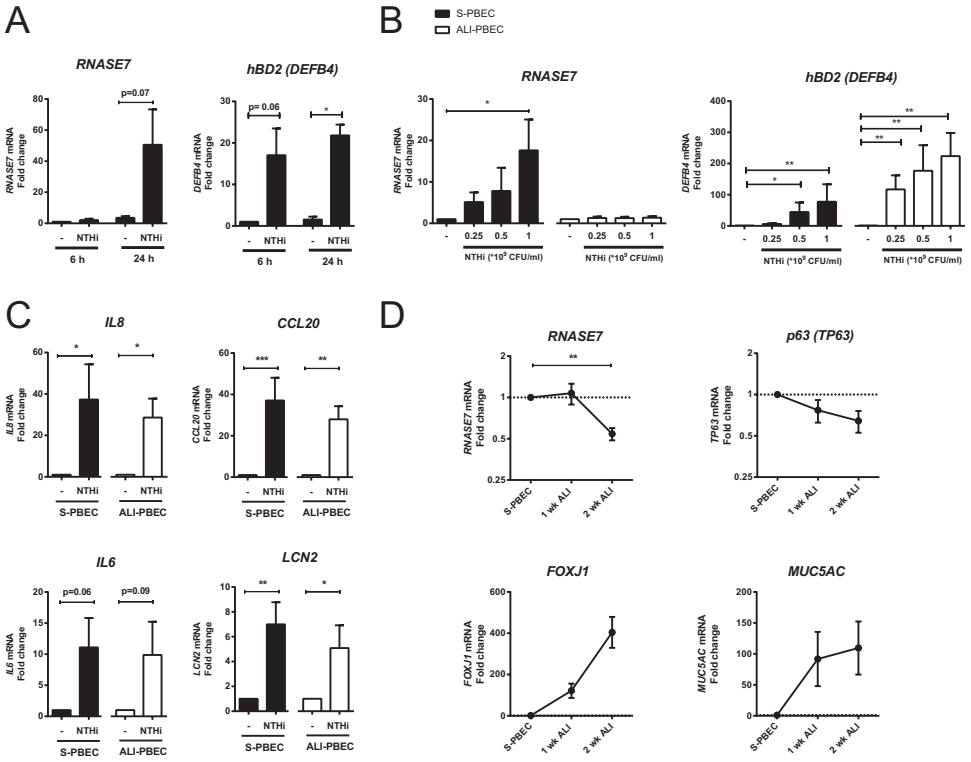

Figure 1. Differential expression of RNase 7 depending on the airway epithelial differentiation status. (A) S-PBEC were stimulated with 1*10^9 CFU/ml UV-inactivated NTHi for 6 and 24 h. mRNA expression of RNase 7 and hBD-2 was determined by qPCR. Data is shown as fold change compared to unstimulated cells (n=4 donors). (B) S-PBEC and ALI-PBEC were stimulated with 0.25, 0.5 and 1*10^9 CFU/ml UV-inactivated NTHi for 24 h. NTHi was stimulated on the apical surface of ALI-PBEC in 100 µl of PBS. mRNA expression of RNase7 and hBD-2 (DEFB4) was subsequently assessed. Data is shown as fold change compared to unstimulated cells (n=5 donors). (C) S-PBEC and ALI-PBEC were stimulated with 0.5*10^9 CFU/ml UV-inactivated NTHi for 24 h. mRNA expression of IL-8, IL-6, CCL20 and LCN2 was subsequently determined. Data is shown as fold change compared to unstimulated cells (n=5 donors). (D) Baseline mRNA expression of RNase 7, the basal cell marker p63 (TP63), ciliated cell marker FOXJ1, and goblet cell marker MUC5AC measured in undifferentiated S-PBEC, 1 wk (1 wk ALI) and 2 wk (2 wk ALI) differentiated ALI-PBEC, all cultured on transwells. Data is shown as fold change compared to undifferentiated cells (n=4 donors). All stimulations were performed in duplicate. * p<0.05, ** p<0.01, *** p< 0,0001.

We therefore examined cigarette smoke–induced injury in ALI-PBEC using a whole cigarette smoke exposure model (Figure 2A). First, the cytotoxic effect of smoke exposure was determined by a LDH release assay (Figure. 2B). No significant increase in LDH release was detected in the basal medium of smoke-exposed cells compared with air controls. However, a significant increase in LDH release was observed in the apical surface wash. Despite this

cytotoxic effect, no significant difference was observed in the TEER of air- and smoke exposed cultures after 24 h (Figure. 2C). In contrast, a significant decrease in TEER was observed in the first 2 h after smoke exposure, indicating transient injury. Further evaluation of the epithelial barrier function by FITC–dextran permeability also confirmed increased barrier disruption in the first 2 h after smoke exposure, whereas no difference in permeability was detected 24 h after exposure (Figure 2D). To examine whether transient epithelial damage induced by cigarette smoke affected the expression of RNase 7, mRNA expression levels were measured at different time periods after exposure. A time-dependent increase in RNase 7 mRNA expression was detected after smoke exposure, which peaked after 3 h and remained significantly different compared with air exposed cells after 6 h (Figure 3A). Similar to increased RNase 7 mRNA expression, protein expression was increased in lysates of ALI-PBEC at 6, 12, and 24 h after smoke exposure (Figure 3B,C). Moreover, increased RNase 7 secretion was measured in the apical surface liquid but not in the basolateral culture medium 24 h after exposure, indicating

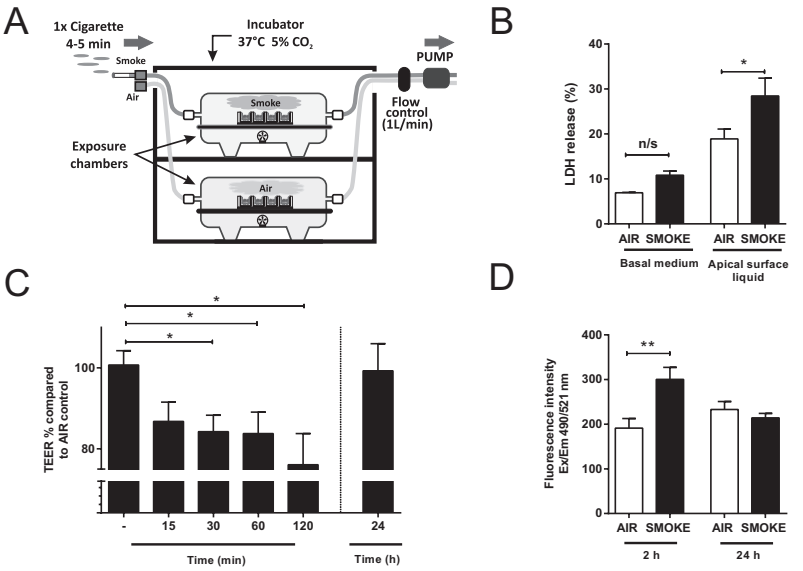

Figure 2. Attenuation of the airway epithelial barrier integrity by whole cigarette smoke exposure. (A) Schematic representation of the whole cigarette smoke exposure model (See materials and methods for details). (B) LDH release was measured in the basal medium 24 h after air/smoke exposure. Data is depicted as percentage cytotoxicity compared to the positive control Triton-X (n=5 donors). (C) Trans-epithelial electrical resistance (TEER) measurements 15-120 minutes and 24 h after air/smoke exposure. Data is shown as percentage compared to TEER measurements of air exposed cells (n=4-9 donors). (D) FITC-dextran was applied on the apical surface either directly or 24 h after air/smoke exposure, and incubated for 2 h. Afterwards the fluorescence was measured in basal medium samples. Data is shown as the measured fluorescence (n=4 donors). All exposures were performed in duplicate. * $p<0.05$, ** $p<0.01$.

polarized secretion of RNase 7 (Figure 3D). We further examined the expression of other mediators besides RNase 7 to delineate the innate immune response induced by cigarette smoke. In contrast to RNase 7, cigarette smoke did not increase mRNA expression of the AMPs hBD-2, hBD-3, LCN2, and Psoriasin/S100A7 (data not shown). However, smoke did induce mRNA expression of IL-8 and IL-6 (Figure 3E), in line with previous observations by others (25). Furthermore, cigarette smoke exposure increased mRNA expression of CCL20, which previously was reported to be induced in airway epithelial cells upon disruption of the airway epithelial barrier integrity (32). In line with mRNA expression, we also detected cigarette smoke–induced IL-8 protein secretion in the basal medium and apical surface liquid (Figure 3F). In summary, we demonstrated that transient injury induced by cigarette smoke exposure is paired with increased expression and polarized secretion of RNase 7 by ALI-PBEC. This response is part of a distinct innate immune response including the expression of IL-8, IL-6, and CCL20, but lacks induction of other AMPs that were investigated.

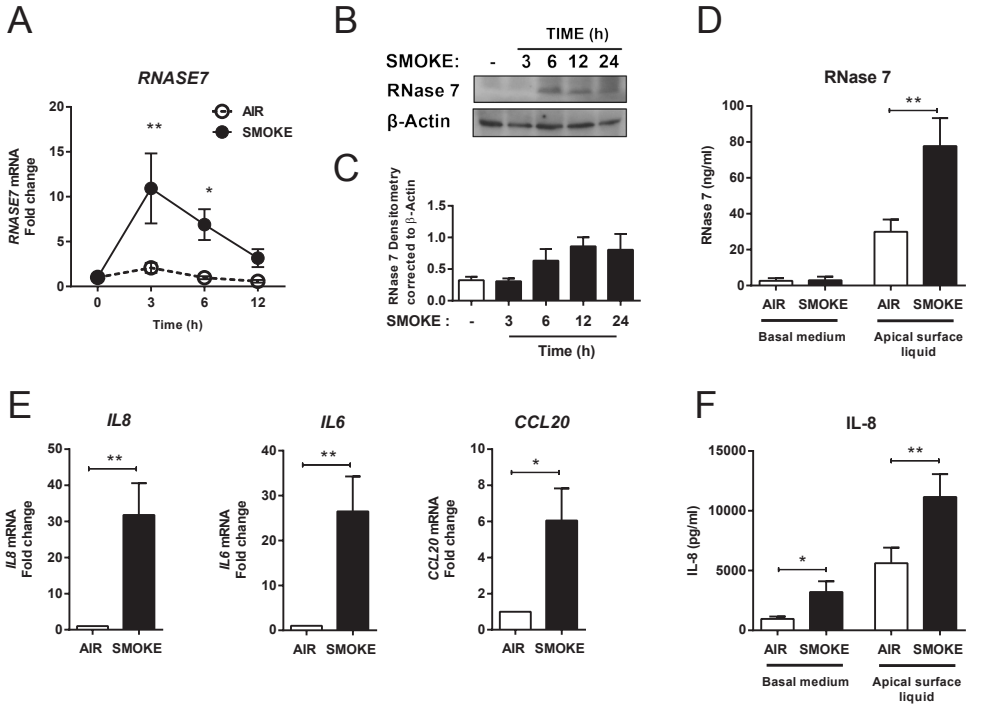

Figure 3. Production of RNase 7 and other innate immune mediators by ALI-PBEC in response to cigarette smoke. (A) ALI-PBEC were exposed to air or cigarette smoke and afterwards incubated for different time periods. mRNA expression levels of RNase 7 was determined by qPCR at 3, 6 and 12 h after air/smoke exposure. Data is shown as fold change compared to unexposed cells (n=6 donors). (B) RNase 7 protein detection in cell lysates of ALI-PBEC, 24 h after air/smoke exposure (data represents 3 independent donors). (C) RNase 7 protein expression was determined by ELISA in the basal medium and apical surface liquid 24 h after air/smoke exposure (n=5 donors). (D) qPCR of IL-8, IL-6 and CCL20, 3 h after air/smoke exposure. Data is shown as fold change compared to air exposed cells (n=6 donors). (E) IL-8 secretion was measured by ELISA in the basal medium and apical surface liquid 24 h after air/smoke exposure (n=6 donors). Air/smoke exposures were performed in duplicate. *p<0.05, ** p<0.01.

Smoke enhances RNase 7 expression specifically in BCs of ALI-PBEC

To determine whether cigarette smoke–induced RNase 7 was specifically expressed by BCs in ALI-PBEC, we analysed mRNA expression in the basal and luminal cell fraction of ALI-PBEC that were separated based on a previous described method (26). To validate the nature of the isolated fractions, we initially examined the mRNA expression of the BC markers p63 and KRT5. Both p63 and KRT5 mRNA levels were significantly higher in the basal fraction compared with the luminal fraction in smoke- and air- exposed cultures (Figure 4A). Interestingly, we observed a significant decrease in p63 and KRT5 mRNA levels in the basal fraction of smoke-exposed cultures. At later time points, these levels returned to baseline levels (*unpublished data*), suggesting that the effect of smoke exposure on these basal cell markers is only transient. In contrast, mRNA expression of RNase 7 was significantly increased 3 h after smoke exposure in the basal fraction, but not in the luminal fraction of ALI-PBEC, whereas smoke-induced mRNA expression of IL-8 was observed in both the basal and the luminal fraction. Examination of RNase 7 protein expression was subsequently determined by assessing co-localization of RNase 7 with p63 using immunofluorescence confocal imaging. Confocal imaging of the apical side of ALI-PBEC lacking $p63^+$ cells, demonstrated that RNase 7 expression could not be observed in both air- and smoke-exposed ALI-PBEC after 6 h (Figure 4B). However, RNase 7 co-localized with $p63^+$ cells at the basal side of ALI-PBEC, which was more abundant in cigarette smoke–exposed cultures than air controls. In these confocal studies, we did not observe a decrease in p63 protein levels or the number of $p63^+$ cells in smoke-exposed cultures compared with air controls, contrasting the observed decreased mRNA expression of p63. To quantify RNase 7 expression in BCs, we performed flow cytometric analysis examining RNase 7 expression in $KRT5^+$ cells in ALI-PBEC, 6 h after air/smoke exposure (Figure 4C). Cigarette smoke significantly increased RNase 7 in the $KRT5^+$ fraction compared with air exposed cultures (Figure 4D), whereas no effect was observed in the $KRT5^-$ fraction. Similar to p63 protein detection by confocal imaging, we did not observed a difference in the ratio of $KRT5^-$ and $KRT5^+$ cells upon smoke exposure (data not shown). Supporting our hypothesis, we observed that smoke exposure induced RNase 7 expression in ALI-PBEC selectively in BCs.

Bacterial stimulation does not further increase cigarette smoke-induced RNase 7 expression

We further evaluated the additional effect of bacterial stimulation on smoke-induced RNase 7 expression. After smoke exposure, ALI-PBEC were stimulated with either NTHi or the TLR2 ligand Pam3CSK4. Consistent with previous studies examining the effect of whole cigarette smoke on bacterial induced expression of IL-8 and hBD-2 (33), cigarette smoke inhibited NTHi- and Pam3CSK4-induced hBD-2 expression while increasing smoke-induced IL-8 mRNA expression (Figure 5). In line with the observation in Figure 1B, NTHi did not induce RNase 7 mRNA expression at 3, 12, and 24 h after exposure (Figure 5A,B). Moreover, NTHi did not further increase smoke-induced RNase 7 mRNA levels. Similar to NTHi, TLR2 activation with Pam3CSK4 did not affect RNase 7 mRNA expression after 3 h of stimulation (Figure 5C).

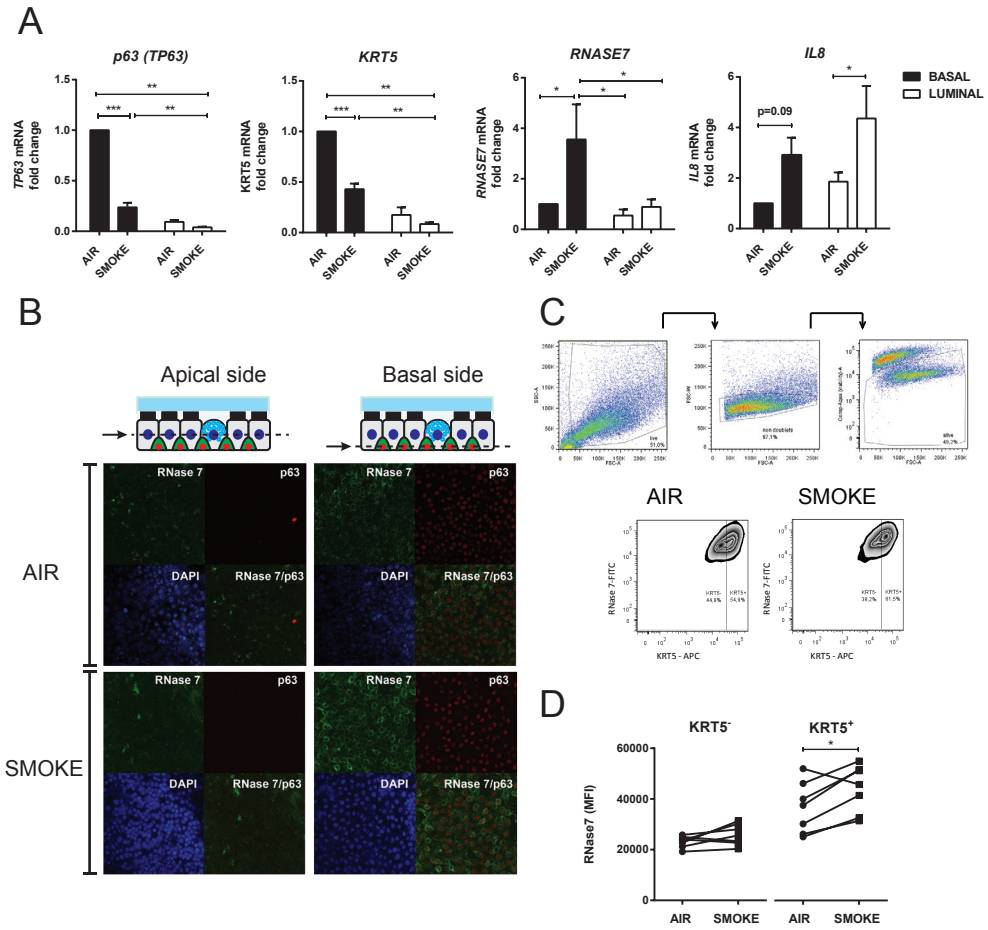

Figure 4. BC-specific expression of RNase 7 in ALI-PBEC after smoke exposure. (A) ALI-PBEC were exposed to air or smoke, and the basal and luminal cell fraction were isolated 3 h after exposure. mRNA expression of p63, KRT5, RNase 7 and IL-8 was determined by qPCR. Data is shown as fold change compared to the air exposed basal fraction (n=4 donors). For protein detection, ALI-PBEC were exposed to air or cigarette smoke, and after 3 h refreshed with culture medium containing 5 µg/ml Brefeldin A to prevent protein secretion. After an additional 3 h, RNase 7 protein localization was determined by confocal imaging and flow cytometry. (B) For confocal imaging, ALI-PBEC were immunostained for RNase 7 (Green) and p63 (Red) and DAPI (Blue). Confocal images were made of the apical site without p63+ cells and basolateral site containing p63+ cells (data represents 3 independent donors). (C) For flow cytometry, ALI-PBEC were detached from the transwell inserts by treatment with soft trypsin and cell suspensions were subsequently stained for RNase 7 and KRT5. Flow cytometric analysis was performed excluding doublets and dead cells by aqua staining. Data is shown as the mean fluorescence intensity (MFI) of the KRT5- and KRT5+ positive fraction (n=6 donors). Air/smoke exposures were performed in duplicate. *p<0.05, ** p<0.01, *** p< 0,0001.

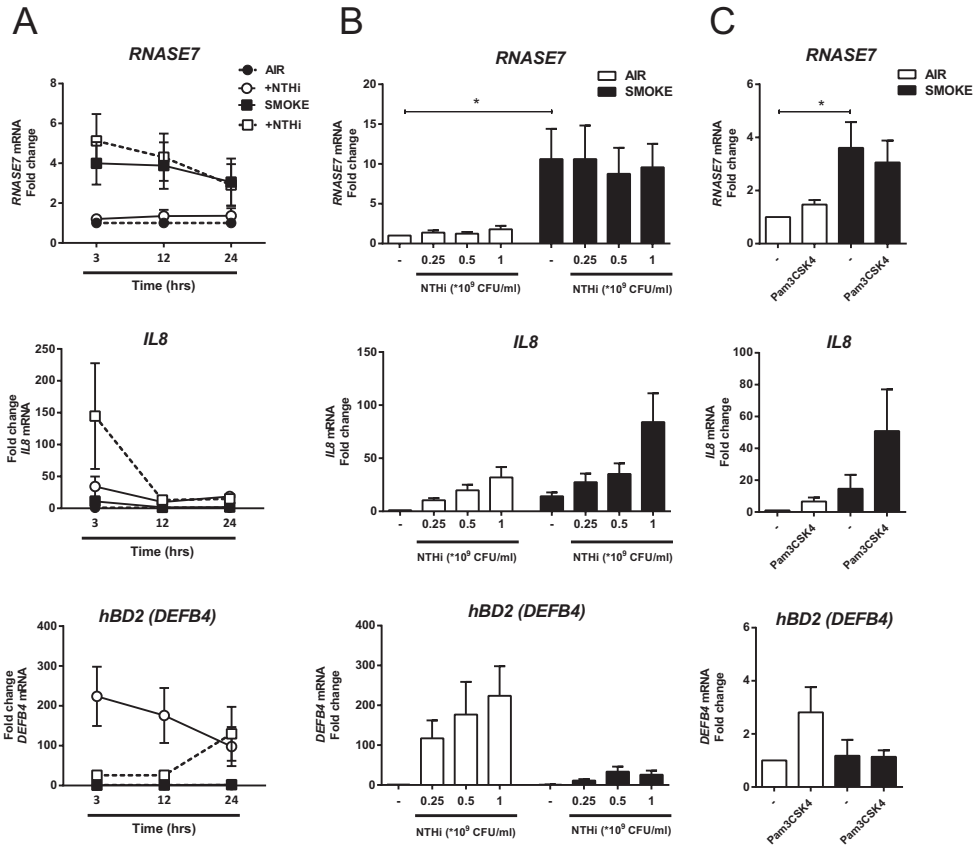

Figure 5. The effect of bacterial stimuli on smoke-induced RNase 7 expression by ALI-PBEC. After air/smoke exposure, (A) ALI-PBEC were stimulated apical with 100 µl of 10*10^7 CFU/ml NTHi for 3, 12 and 24 h (n=6 donors), (B) 100 µl of different concentrations of NTHi (0.25, 0.5 and 1 *10^9 CFU/ml) for 3 h (n=6 donors) or (C) Pam3CSK4 (1 µg/ml) for 4 h (n=5 donors). RNase 7, IL-8 and hBD-2 mRNA expression was assessed by qPCR. Data is shown as fold change compared to air exposed cells. All stimulations were performed in duplicate. *p<0.05.

Cigarette smoke–induced RNase 7 expression requires activation of the epidermal growth factor receptor

Airway epithelial BCs are characterized by selective expression of the EGFR, a receptor that is activated upon disruption of the epithelial barrier function by cigarette smoke (31, 34). Previous studies reported that cigarette smoke extract induced expression of IL-8 in airway epithelial cells, which required activation of EGFR and the downstream MAPK/ERK 1/2 (ERK1/2) (35, 36). Therefore, we studied whether EGFR and ERK1/2 signalling were required in cigarette smoke–induced expression of RNase 7. Our results clearly showed that similar to cigarette smoke extract, whole cigarette smoke exposure increased phosphorylation of EGFR and ERK1/2 in ALI-PBEC 15 min after exposure (Figure 6A,B). Inhibition of EGFR using a neutralizing Ab, the EGFR tyrosine kinase inhibitor AG1478, and the ERK1/2-activating kinases MEK1/2 inhibitor U0126, attenuated activation of ERK1/2, demonstrating that indeed smoke activates ERK1/2 in an EGFR dependent manner. Pharmacological inhibition

of EGFR with AG1478 and inhibition of the ERK1/2-activating kinases MEK1/2 with U0126 caused a significant decrease in smoke-induced mRNA expression of RNase 7 (Figure 6C). Similar to RNase 7, and in line with previous studies, mRNA expression of IL-8 and CCL20 was also impaired upon inhibition of EGFR and MEK/ERK1/2, while a trend was observed for IL-6 expression. To further support the conclusion that EGFR activation mediates RNase 7 expression, we examined the effect of direct receptor activation by stimulating ALI-PBEC with TGF-α. Indeed, in line with the effect of cigarette smoke, 3 h stimulation with TGF-α

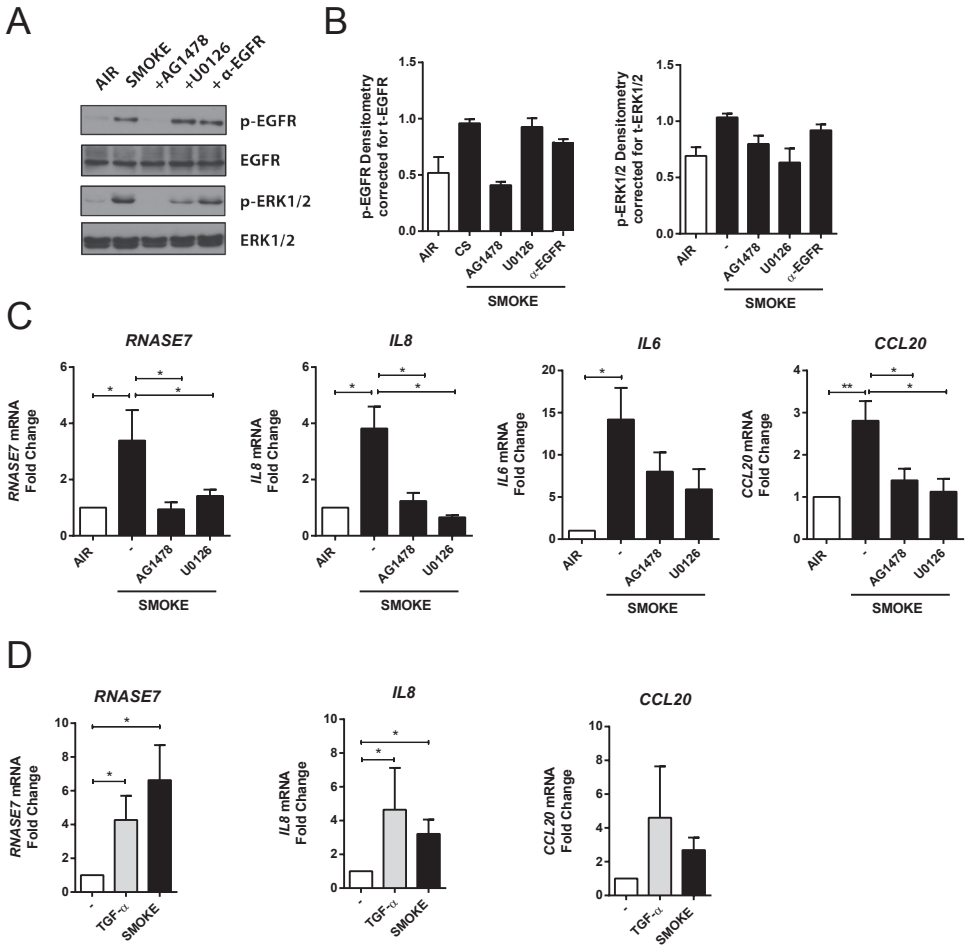

Figure 6. Requirement of EGFR and ERK1/2 in cigarette smoke induced RNase 7 expression by ALI-PBEC. (A) ALI-PBEC were pre-incubated for 1 h with AG1478 (EGFR inhibitor; 1 μM) or EGFR neutralizing antibody (2 μg/ml), prior to smoke exposure. Western blot analysis was performed of p-EGFR, p-ERK1/2 15 minutes after air/smoke exposure. Total EGFR and ERK1/2 were used as loading controls (data represents 3 independent donors). (B) PBEC were pre-incubated for 1 h with AG1478 (EGFR inhibitor; 1 μM) or U0125 (MEK1/2 inhibitor; 25 μM) prior to air/smoke exposure. RNase 7, IL-8, IL-6 and CCL20 mRNA expression was assessed 3 h after exposure by qPCR. Data is shown as fold change compared to air exposed cells (n=6). * $p<0.05$.

significantly enhanced RNase 7 mRNA expression and furthermore increased IL-8 expression; the increase in CCL20 did not reach statistical significance (Figure 6D). In conclusion, we observed that cigarette smoke–induced expression of RNase 7 requires activation of the BC-specific receptor EGFR and the downstream ERK1/2 signalling pathway.

DISCUSSION

In this study, we examined the expression of the antimicrobial RNase 7 in cultured airway epithelial cells. We demonstrated that undifferentiated S-PBEC, primarily consisting of BCs, but not mucociliary-differentiated ALI-PBEC, expressed RNase 7 upon stimulation with the respiratory pathogen NTHi. This was in marked contrast to other examined innate immune mediators that were induced by NTHi in both S-PBEC and ALI-PBEC. Furthermore, differentiated ALI-PBEC displayed a decreased baseline RNase 7 expression compared with S-PBEC after 2 wk of culturing in air-exposed conditions. Cigarette smoke exposure, which caused transient disruption of the epithelial barrier function, reinitiated RNase 7 expression in the remaining undifferentiated BCs in ALI-PBEC, which was demonstrated using confocal microscopy and isolation of luminal and basal cell fractions. Moreover, we showed that this induction required activation of EGFR and the downstream ERK1/2 signalling pathway and furthermore demonstrated that direct EGFR activation by TGF-α also induced RNase 7 expression. In contrast to the innate immune mediators IL-8 and hBD-2, bacterial co-stimulation did not further affect smoke-induced RNase 7 expression in ALI-PBEC. This data suggest that expression of RNase 7 is a unique innate host defence property of BCs that is induced in conditions of airway epithelial injury. To our knowledge, we demonstrate for the first time that BCs display a phenotype-distinct antimicrobial response by producing RNase 7. The epithelial phenotype–specific expression of AMPs has been well described in multiple mucosal tissues (37). For instance, intestinal Paneth cells selectively produce human α-defensin 5 and 6, which are not produced by enterocytes (38). In the lung, phenotype-specific expression of AMPs has been observed in submucosal gland serous cells, which produce lactoferrin and lysozyme (39, 40) and also in alveolar cells producing antimicrobial surfactant protein A and D (41). Phenotype-specific expression of RNase 7 has been reported in the skin and urinary tract, demonstrating specific expression by respectively suprabasal keratinocytes and α- and β-intercalated cells (16, 18). In contrast to these epithelial cells, phenotype-distinct expression of AMPs by airway epithelial BCs has not yet been reported. Similar to previous in vitro observations demonstrating BC specific expression of IL-33 and EGFR (10, 34), we observed decreased expression of RNase 7 after mucociliary differentiation of PBEC. Consistent with this observation, it was shown in a previous transcriptome analysis that RNase 7 transcripts were increased in BCs but not in differentiated airway epithelial cells (28). Another transcriptome analysis demonstrated enhanced mRNA expression of RNase 1, 4, and 6 in differentiated airway epithelial cells compared with undifferentiated cultures (42), suggesting that RNase 7 production by BCs is unique among other secreted RNases. Interestingly, we did not observe a difference in RNase 7 mRNA expression after 1 wk of mucociliary differentiation of ALI-PBEC. As the amount of BCs declines during the first week of differentiation, we reasoned that the attenuation of RNase 7 expression after 2 wk of differentiation was not caused by a decrease in the number of BCs in cultured ALI-PBEC but because of another mechanism. Because undifferentiated ALI-PBEC initially display a low epithelial barrier function that progresses during differentiation, we hypothesized that RNase

7 expression by BCs in ALI-PBEC is attenuated because of an enhanced airway epithelial barrier function. Our finding that cigarette smoke can reinitiate RNase 7 expression by BCs in ALI-PBEC supported this hypothesis. Previous data demonstrate that E-cadherin–mediated cell–cell contacts inhibit EGFR signalling in airway epithelial cells (43). Because we observed that cigarette smoke decreases epithelial barrier function, which has been shown to be related to interference with the function of E-cadherin (30), and because smoke-induced RNase 7 expression involved EGFR activation, we reason that smoke-induced barrier disruption contributes to RNase 7 expression. In skin host defence, it is well established that injury enhances EGFR-dependent innate immune responses by keratinocytes that provide protection against infections during wound repair (44, 45). Also, in airway epithelial cells, it has been shown that EGFR activation promotes innate immune responses that are depending on the MAPK/ERK1/2 signalling pathway, which also facilitates epithelial wound healing (36, 46). These studies primarily demonstrate EGFR-dependent expression of pro-inflammatory innate immune mediators such as IL-8, IL-6, and CCL20, which were also induced by cigarette smoke in our model. However, to our knowledge, this is the first study reporting EGFR-dependent AMP expression in airway epithelial cells. Although smoke-induced RNase 7 expression was specifically detected in BCs, we observed secretion of RNase 7 in the apical surface liquid. This may be the result of polarized secretion to the apical side, which can be mediated in part by trans-epithelial projections between the lateral intracellular spaces formed by BCs (47). These projections might explain the apical secretion of RNase 7. However, this requires further investigation. Besides decreased baseline RNase 7 expression in ALI-PBEC, we furthermore demonstrated that in contrast to S-PBEC, ALI-PBEC did not induce RNase 7 expression after stimulation with NTHi. Also, additional stimulation with NTHi or the TLR2 ligand Pam3CSK4 did not further enhance cigarette smoke–induced RNase 7 expression, whereas expression of IL-8 was further increased. It can be speculated that the inability of bacterial stimuli to induce RNase 7 expression in BCs of ALI-PBEC is caused by a lack of direct microbial contact of BCs because of apical application of the NTHi and Pam3CSK4. Similar to the pseudostratified airway epithelium *in vivo*, undifferentiated BCs in cultured ALI-PBEC are superimposed by differentiated LCs. In intact airway epithelium, this mechanism might protect BCs from direct microbial contact and subsequently prevents RNase 7 expression. Another explanation of the absence of bacterial induced RNase 7 expression in BCs of ALI-PBEC might be that pattern recognition receptors such as TLR2 are localized at the basolateral site of BCs because of cell polarization. Finally, we cannot formally exclude the possibility that, in contrast to UV-inactivated bacteria, life-NTHi may promote RNase 7 expression in basal cells *in vivo* (e.g., as a result of epithelial barrier disruption). In contrast to RNase 7, NTHi-induced hBD-2 in airway epithelial cells was independent of the epithelial differentiation status. Furthermore, cigarette smoke exposure impaired bacterial-induced hBD-2 (33). This finding is in line with a decreased antimicrobial defence of airway epithelial cells exposed to cigarette smoke, which provides an explanation for the increased susceptibility of smokers and chronic obstructive pulmonary disease patients toward respiratory infections (33). We argue that the decreased antimicrobial defence caused by smoking results from the attenuation of a large number of AMPs including hBD-2, which cannot be compensated by RNase 7 expression. To further explore the significance of RNase 7 in airway epithelial host defence upon barrier disruption, other environmental factors should be examined that affect the epithelial barrier function but do not attenuate the expression of other AMPs. On the basis of our observations, we propose a novel model of

airway epithelial host defence that includes a second line of defense mediated by airway BCs, which is induced upon injury. In the intact airway epithelium, LCs are the main cells that mediate host defence via, for example, production of AMPs such as hBD-2 and mucociliary clearance (Figure 7A). LCs furthermore prevent microbial contact of the basolateral localized BCs, thereby preventing RNase 7 expression. However, BCs do produce RNase 7 upon disruption of the epithelial barrier integrity by inhaled substances such as cigarette smoke (Figure 7B). Moreover, in damaged epithelium lacking LCs, microbial exposure of BCs induces innate immune responses including cell type–specific expression of RNase 7. This way BCs provide additional innate immune defence against microbial infections during the course of epithelial wound repair.

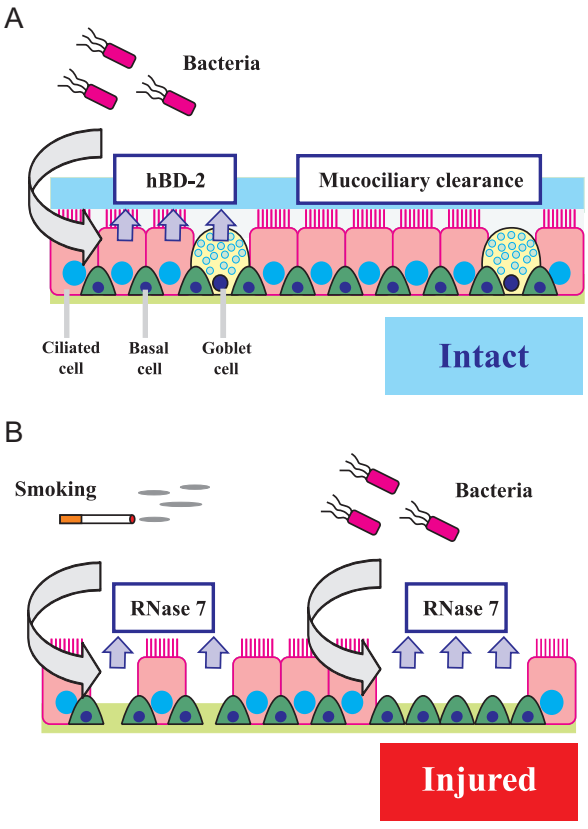

Figure 7. Proposed model. (A) Innate host defense of undamaged airway epithelium mediated by LCs containing ciliated and secretory/goblet cells, for instance providing protection against bacteria via production of hBD-2 and mucociliary clearance. (B) Second line of airway epithelial innate host defense upon injury mediated by BCs, which selectively producing RNase 7. Expression of RNase 7 is induced upon disruption of the epithelial barrier caused by cigarette smoking or upon bacterial exposure in regions lacking LCs.

ACKNOWLEDGMENTS

We thank Jerry van der Ploeg (Department of Instrumental Services, Leiden University Medical Center) for technical assistance in developing the whole cigarette smoke exposure model. We also thank Dr. Joop Wiegant, (Department of Molecular Cell Biology, Leiden University Medical Center) for technical expertise using the Leica TCS SP5 Confocal Microscope, and Sanne de Jong (Department of Parasitology, Leiden University Medical Center) for help with the flow cytometry analysis. We furthermore thank Dr. Jamil Aarbiou (Galapagos BV, the Netherlands) for helpful discussion.

REFERENCES

1. Bals R, Hiemstra PS. Innate immunity in the lung: how epithelial cells fight against respiratory pathogens. European Respiratory Journal. 2004;23(2):327-33.
2. Hallstrand TS, Hackett TL, Altemeier WA, Matute-Bello G, Hansbro PM, Knight DA. Airway epithelial regulation of pulmonary immune homeostasis and inflammation. Clinical Immunology. 2014;151(1):1-15.
3. Knowles MR, Boucher RC. Mucus clearance as a primary innate defense mechanism for mammalian airways. The Journal of Clinical Investigation. 2002;109(5):571-7.
4. Kesimer M, Ehre C, Burns KA, Davis CW, Sheehan JK, Pickles RJ. Molecular organization of the mucins and glycocalyx underlying mucus transport over mucosal surfaces of the airways. Mucosal Immunol. 2013;6(2):379-92.
5. Soong G, Reddy B, Sokol S, Adamo R, Prince A. TLR2 is mobilized into an apical lipid raft receptor complex to signal infection in airway epithelial cells. The Journal of Clinical Investigation. 2004;113(10):1482-9.
6. Gohy ST, Detry BR, Lecocq Mn, Bouzin C, Weynand BA, Amatngalim GD, et al. Polymeric Immunoglobulin Receptor Downregulation in COPD: Persistence in the Cultured Epithelium and Role of Transforming Growth Factor-b. American Journal of Respiratory and Critical Care Medicine; 7/31/2014: American Thoracic Society - AJRCCM; 2014.
7. Rock JR, Hogan BLM. Epithelial Progenitor Cells in Lung Development, Maintenance, Repair, and Disease. Annual Review of Cell and Developmental Biology; 10/10/2011: Annual Reviews; 2011. p. 493-512.
8. Teixeira VH, Nadarajan P, Graham TA, Pipinikas CP, Brown JM, Falzon M, et al. Stochastic homeostasis in human airway epithelium is achieved by neutral competition of basal cell progenitors. eLife. 2013;2.
9. Rock JR, Onaitis MW, Rawlins EL, Lu Y, Clark CP, Xue Y, et al. Basal cells as stem cells of the mouse trachea and human airway epithelium. Proceedings of the National Academy of Sciences. 2009;106(31):12771-5.
10. Byers DE, Alexander-Brett J, Patel AC, Agapov E, Dang-Vu G, Jin X, et al. Long-term IL-33-producing epithelial progenitor cells in chronic obstructive lung disease. The Journal of Clinical Investigation. 2013;123(9):3967-82.
11. Ganz T. Antimicrobial polypeptides in host defense of the respiratory tract. The Journal of Clinical Investigation. 2002;109(6):693-7.
12. Zasloff M. Antimicrobial peptides of multicellular organisms. Nature. 2002;415(6870):389.
13. Hilchie A, Wuerth K, Hancock R. Immune modulation by multifaceted cationic host defense (antimicrobial) peptides. Nature chemical biology. 2013;9(12):761-8.
14. Harder J, Schröder JM. RNase 7, a Novel Innate Immune Defense Antimicrobial Protein of Healthy Human Skin. Journal of Biological Chemistry. 2002;277(48):46779-84.
15. Zhang J, Dyer KD, Rosenberg HF. Human RNase 7: a new cationic ribonuclease of the RNase A superfamily. Nucleic Acids Research. 2003;31(2):602-7.
16. Köten B, Simanski M, Gläser R, Podschun R, Schröder JM, Harder J. RNase 7 Contributes to the Cutaneous Defense against Enterococcus faecium. PLoS ONE. 2009;4(7):e6424.
17. Mun J, Tam C, Chan G, Kim JH, Evans D, Fleiszig S. MicroRNA-762 Is Upregulated in Human Corneal Epithelial Cells in Response to Tear Fluid and Pseudomonas aeruginosa Antigens and Negatively Regulates the Expression of Host Defense Genes Encoding RNase7 and ST2. PLoS ONE. 2013;8(2):e57850.
18. Spencer JD, Schwaderer AL, DiRosario JD, McHugh KM, McGillivary G, Justice SS, et al. Ribonuclease 7 is a potent antimicrobial peptide within the human urinary tract. Kidney Int. 2011;80(2):174-80.
19. Simanski M, Dressel S, Glaser R, Harder J. RNase 7 Protects Healthy Skin from Staphylococcus aureus Colonization. J Invest Dermatol. 2010;130(12):2836-8.
20. Gläser R, Navid F, Schuller W, Jantschitsch C, Herr C, Harder J, et al. UV-B radiation induces the expression of antimicrobial peptides in human keratinocytes in vitro and in vivo. Journal of Allergy and Clinical Immunology. 2009;123(5):1117-23.
21. Harder J, Dressel S, Wittersheim M, Cordes J, Meyer-Hoffert U, Mrowietz U, et al. Enhanced Expression and

Secretion of Antimicrobial Peptides in Atopic Dermatitis and after Superficial Skin Injury. J Invest Dermatol. 2010;130(5):1355-64.

22. van Wetering S, van der Linden AC, van Sterkenburg MAJA, Rabe KF, Schalkwijk J, P.S. H. Regulation of secretory leukocyte proteinase inhibitor (SLPI) production by human bronchial epithelial cells: increase of cell-associated SLPI by neutrophil elastase. Journal of investigative medicine. 2000;48(5):359-66.

23. van Wetering S, Zuyderduyn S, Ninaber DK, van Sterkenburg MAJA, Rabe KF, Hiemstra PS. Epithelial differentiation is a determinant in the production of eotaxin-2 and -3 by bronchial epithelial cells in response to IL-4 and IL-13. Molecular Immunology. 2007;44(5):803-11.

24. Groeneveld K, van Alphen L, Eijk PP, Visschers G, Jansen HM, Zanen HC. Endogenous and Exogenous Reinfections by Haemophilus influenzae in Patients with Chronic Obstructive Pulmonary Disease: The Effect of Antibiotic Treatment on Persistence. Journal of Infectious Diseases. 1990;161(3):512-7.

25. Beisswenger C, Platz J, Seifart C, Vogelmeier C, Bals R. Exposure of Differentiated Airway Epithelial Cells to Volatile Smoke in vitro. Respiration. 2004;71(4):402-9.

26. Jakiela B, Brockman-Schneider R, Amineva S, Lee WM, Gern JE. Basal Cells of Differentiated Bronchial Epithelium Are More Susceptible to Rhinovirus Infection. American Journal of Respiratory Cell and Molecular Biology; 5/1/2008: American Thoracic Society - AJRCMB; 2008. p. 517-23.

27. Luppi F, Aarbiou J, van Wetering S, Rahman I, de Boer W, Rabe K, et al. Effects of cigarette smoke condensate on proliferation and wound closure of bronchial epithelial cells in vitro: role of glutathione. Respiratory Research. 2005;6(1):140.

28. Hackett NR, Shaykhiev R, Walters MS, Wang R, Zwick RK, Ferris B, et al. The Human Airway Epithelial Basal Cell Transcriptome. PLoS ONE. 2011;6(5):e18378.

29. Dvorak A, Tilley AE, Shaykhiev R, Wang R, Crystal RG. Do Airway Epithelium Air-Liquid Cultures Represent the In Vivo Airway Epithelium Transcriptome? American Journal of Respiratory Cell and Molecular Biology; 4/1/2011: American Thoracic Society - AJRCMB; 2011. p. 465-73.

30. Heijink IH, Brandenburg SM, Postma DS, van Oosterhout AJM. Cigarette smoke impairs airway epithelial barrier function and cell-cell contact recovery. European Respiratory Journal. 2012;39(2):419-28.

31. Petecchia L, Sabatini F, Varesio L, Camoirano A, Usai C, Pezzolo A, et al. Bronchial airway epithelial cell damage following exposure to cigarette smoke includes disassembly of tight junction components mediated by the extracellular signal-regulated kinase 1/2 pathway. CHEST Journal. 2009;135(6):1502-12.

32. Post S, Nawijn MC, Hackett TL, Baranowska M, Gras R, van Oosterhout AJM, et al. The composition of house dust mite is critical for mucosal barrier dysfunction and allergic sensitisation. Thorax. 2012;67(6):488-95.

33. Herr C, Beisswenger C, Hess C, Kandler K, Suttorp N, Welte T, et al. Suppression of pulmonary innate host defence in smokers. Thorax. 2009;64(2):144-9.

34. Shaykhiev R, Zuo WL, Chao I, Fukui T, Witover B, Brekman A, et al. EGF shifts human airway basal cell fate toward a smoking-associated airway epithelial phenotype. Proceedings of the National Academy of Sciences. 2013;110(29):12102-7.

35. Richter A, O'Donnell RA, Powell RM, Sanders MW, Holgate ST, Djukanovic R. Autocrine ligands for the epidermal growth factor receptor mediate interleukin-8 release from bronchial epithelial cells in response to cigarette smoke. Am J Respir Cell Mol Biol. 2002;27(1):85-90.

36. Burgel PR, Nadel JA. Epidermal growth factor receptor-mediated innate immune responses and their roles in airway diseases. European Respiratory Journal. 2008;32(4):1068-81.

37. Gallo RL, Hooper LV. Epithelial antimicrobial defence of the skin and intestine. Nat Rev Immunol. 2012;12(7):503-16.

38. Ouellette AJ. Paneth cell a-defensins in enteric innate immunity. Cell Mol Life Sci
Cellular and Molecular Life Sciences; 2011: SP Birkh+ñuser Verlag Basel; 2011. p. 2215-29.

39. Bowes D, Corrin B. Ultrastructural immunocytochemical localisation of lysozyme in human bronchial glands.

Thorax. 1977;32(2):163-70.
40. Bowes D, Clark AE, Corrin B. Ultrastructural localisation of lactoferrin and glycoprotein in human bronchial glands. Thorax. 1981;36(2):108-15.
41. Wu H, Kuzmenko A, Wan S, Schaffer L, Weiss A, Fisher JH, et al. Surfactant proteins A and D inhibit the growth of Gram-negative bacteria by increasing membrane permeability. The Journal of Clinical Investigation. 2003;111(10):1589-602.
42. Ross AJ, Dailey LA, Brighton LE, Devlin RB. Transcriptional Profiling of Mucociliary Differentiation in Human Airway Epithelial Cells. American Journal of Respiratory Cell and Molecular Biology; 8/1/2007: American Thoracic Society - AJRCMB; 2007. p. 169-85.
43. Heijink IH, Kies PM, Kauffman HF, Postma DS, van Oosterhout AJM, Vellenga E. Down-Regulation of E-Cadherin in Human Bronchial Epithelial Cells Leads to Epidermal Growth Factor Receptor-Dependent Th2 Cell-Promoting Activity. The Journal of Immunology. 2007;178(12):7678-85.
44. Sorensen OE, Thapa DR, Markus K, Valore EV, bring U, Roberts AA, et al. Injury-induced innate immune response in human skin mediated by transactivation of the epidermal growth factor receptor. The Journal of Clinical Investigation. 2006;116(7):1878-85.
45. Roupe KM, Nybo M, Sjobring U, Alberius P, Schmidtchen A, Sorensen OE. Injury Is a Major Inducer of Epidermal Innate Immune Responses during Wound Healing. J Invest Dermatol. 2010;130(4):1167-77.
46. Kim S, Lewis C, Nadel JA. CCL20/CCR6 Feedback Exaggerates Epidermal Growth Factor Receptor-Dependent MUC5AC Mucin Production in Human Airway Epithelial (NCI-H292) Cells. The Journal of Immunology. 2011;186(6):3392-400.
47. Shum WWC, Da Silva N, McKee M, Smith PJS, Brown D, Breton S. Transepithelial Projections from Basal Cells Are Luminal Sensors in Pseudostratified Epithelia. Cell. 2008;135(6):1108-17.

SUPPLEMENTARY FIGURES

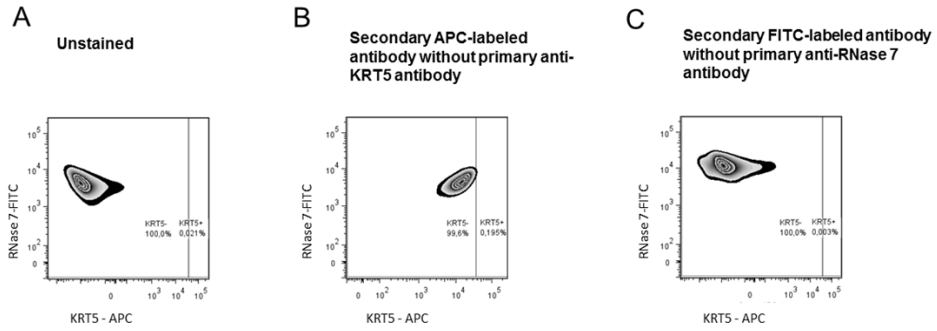

Supplementary Figure 1. Controls FACS analysis. (A) Unstained sample. (B) Staining with the secondary APC-labeled antibody in the absence of the KRT5-specific primary antibody. (C) Staining with the secondary FITC-labeled antibody in the absence of the RNase 7-specific antibody.